

Sharing of vacancies between closely matched *K* and *L* shells

E. M. Middlesworth, Jr.,* D. J. Donahue, L. C. McIntyre, Jr., and E. M. Bernstein†

Department of Physics, University of Arizona, Tucson, Arizona 85721

(Received 2 August 1977)

The sharing of vacancies in the $3d\sigma$ molecular orbital between the *K* shells of chlorine and argon projectiles and $2p_{3/2}$ and $2p_{1/2}$ *L* subshells of tin, antimony, and xenon targets has been studied. Projectile energies varied from 1 to 16 MeV. The vacancy-sharing ratios deduced from experimental results are interpreted in terms of a long-range exponential-coupling model.

I. INTRODUCTION

Level-matching effects have been observed previously in projectile- and target-atom vacancy-production cross sections during heavy-ion-atom collisions.^{1,2} Meyerhof³ has successfully interpreted the vacancy-sharing ratios observed between two matching *K* shells using the long-range exponential-coupling model of Demkov⁴ and the quasimolecular model proposed by Barat and Lichten.⁵ However, in a recent paper, Meyerhof *et al.*⁶ have indicated that to explain vacancy sharing between *K* and *L* shells a more general interpretation using the long-range exponential-coupling model proposed by Nikitin⁷ is necessary. In this paper we describe a series of measurements of *K-L* vacancy ratios. All of the collisions studied here are of the so-called "swapped" type; that is, the binding energy of the *K* shell of the low-*Z* collision partner is less than the binding energy of the *L* shell of the high-*Z* partner. Interpretations of these measurements are discussed.

II. METHOD

Multiply and singly charged ions of chlorine and argon were accelerated to energies ranging from 1 to 16 MeV using a Van de Graaff accelerator. Solid targets of tin and antimony with thicknesses of 30 and 27 $\mu\text{g}/\text{cm}^2$, respectively, were produced by vacuum evaporation onto 6- $\mu\text{g}/\text{cm}^2$ carbon backings. The production of vacancies in the beam ions by the carbon backing was experimentally demonstrated to be negligible compared to the number of vacancies produced by the tin and antimony. A xenon gas target, 0.7 cm thick at a pressure of 7.7 Torr, was provided by a gas cell with a 500- $\mu\text{g}/\text{cm}^2$ nickel entrance window. The geometry was such that inner-shell vacancies produced in the beam atoms by the nickel foil decayed without being observed, and the outer-shell configuration of the beam atoms in the region of observation was determined by equilibrium conditions in the gas. A description of the experi-

mental arrangement is given in Ref. 8.

The x rays emitted from the filling of target *L*-shell vacancies and projectile *K*-shell vacancies were observed with a lithium-drifted silicon detector which has a full-width-at-half-maximum

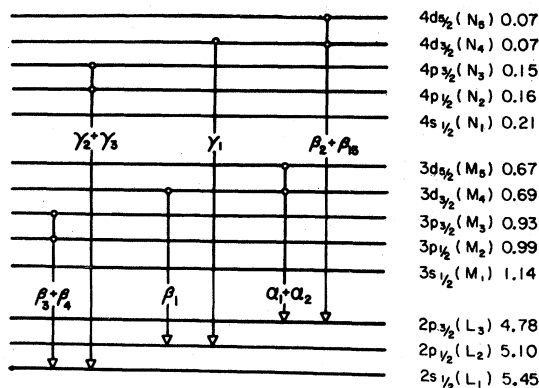
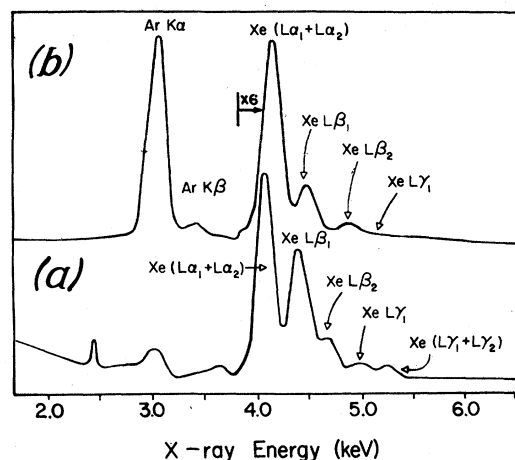


FIG. 1. Spectra of x rays from xenon bombarded by (a) 4-MeV protons and (b) 11-MeV argon ions. Also shown is an energy-level diagram for neutral xenon. Observed transitions are indicated and binding energies are given in keV.

(FWHM) energy resolution of 180 eV. Spectra of x rays emitted in collisions of argon ions and protons with xenon gas are shown in Fig. 1. Also included in Fig. 1 is a diagram showing the energy levels involved in the observed xenon transitions. X rays to vacancies in the $L_1(2S_{1/2})$, $L_2(2P_{1/2})$, and $L_3(2P_{3/2})$ levels of the heavy collision partner are resolved by the Si(Li) detector, and we treat cross sections for production of vacancies in these levels separately. If the vacancies are produced by a transfer of vacancies from the $3d\sigma$ molecular orbital to the L levels, cross sections for production of three types of L -level vacancies will be different. In attempting to interpret the data presented in this paper, we assume that the sharing between the $3d\sigma$ orbital and the three L levels can be treated as three separate two-state problems. A diagram, constructed according to the method of Eichler *et al.*,⁹ and showing the molecular orbitals which are involved in the collisions studied here, but without the spin-orbit splitting of the $2P$ shell, is shown in Fig. 2.

The yield of x rays filling vacancies in the $L_3(2P_{3/2})$ level of Xe was determined from the sum of the areas of peaks in the upper curve labeled $L\alpha_1 + L\alpha_2$ and $L\beta_2$. The yield of x rays to the $L_2(2P_{1/2})$ level was obtained from peaks labeled $L\beta_1$ and $L\gamma_1$. Limits to the yield of x rays to the $L_1(2S_{1/2})$ level were measured through the peak $L\gamma_2 + L\gamma_3$ in the figure. This peak is difficult to see in the Ar+Xe spectrum. From the area or limit to the area of the $L\gamma_2 + L\gamma_3$ peak, and using the ratio $Y(L\gamma_2 + L\gamma_3)/Y(L\gamma_3 + L\gamma_4) = 0.2$,¹⁰ we de-

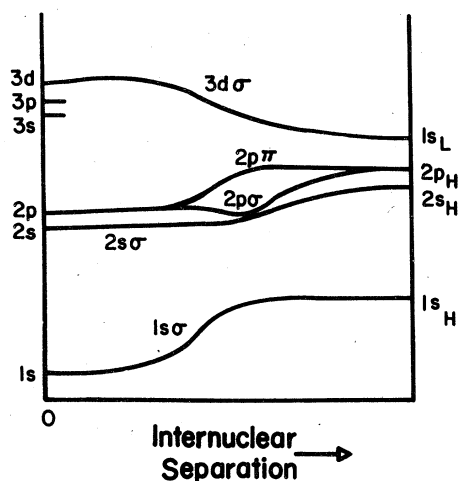


FIG. 2. Partial schematic multiple-electron correlation diagram for atomic collision systems which satisfy the binding-energy condition $(BE)_{2p_H} > (BE)_{1s_L} > (BE)_{3s_H}$ (a "swapped" system).

termined that the vacancy population of the L_1 level is less than $\frac{1}{10}$ of that of the L_2 level, and that the contribution of x rays $L\beta_3$ and $L\beta_4$ (which cannot be resolved from $L\beta_1$) to the peak labeled $L\beta_1$, which is used to obtain the yield of $2P_{1/2}$ -level vacancies, is less than $\frac{1}{10}$ of that peak. Because of the low yield of $L\gamma_2 + L\gamma_3$ x rays, no results were obtained in this work for cross sections for production of $2S_{1/2}$ vacancies in target atoms.

Finally, the yield of K x rays from projectile ions was determined from the sum of the areas of $K\alpha$ and $K\beta$ peaks similar to those shown in Fig. 1. All peak areas were obtained from computer fits of Gaussian curves to the data. The observed x-ray yields were corrected for absorption in the targets and in the beryllium entrance window of the Si(Li) detector, using the absorption coefficients of Veigele.¹¹

To convert the measured x-ray yields to K - or L -shell vacancy yields, consideration must be given to fluorescence yields of the K and L shells and Coster-Kronig transitions among the L subshells. Measurements of energies of K x rays from the argon and chlorine projectiles, when compared to Hartree-Fock calculations of these energies, indicated the existence during the collisions of multiple vacancies in the inner shells of the projectiles. To account for the effect of these vacancies, corrections were made to the single-vacancy fluorescence yields of Bambynek *et al.*,¹² using the techniques of McGuire¹³ and Larkin.¹⁴ Configurations of multiple vacancies cannot always be uniquely determined from the measurement of x-ray energies. For example, energies of K x rays from ions with two $2P$ and two $2S$ vacancies can not be distinguished from those ions with three $2P$ and one $2S$ vacancies. However, corrections to single-vacancy fluorescence yields are nearly the same for these two configurations. The correction factors applied to single-vacancy values of fluorescence yields varied from 1.05 at low energies to 1.35 at the highest energies for projectiles incident on solid targets. For particles incident on gaseous targets, it was necessary to apply a correction factor of 1.35 at all energies. Corrected fluorescence yields were then used to convert K x-ray production rates to K -shell vacancy production rates.

We next consider Coster-Kronig transitions among the L subshells of the target atoms. As mentioned above, the number of x rays from the filling of the L_3 level is greater than that from the filling of the L_2 level, which is in turn greater than the number of x rays from the filling of the L_1 level. Combining these x-ray yields with the single-vacancy Coster-Kronig transition rates given by Bambynek *et al.*,¹² we have concluded

that the observed $L_3(2P_{3/2})$ level yield has a Coster-Kronig contribution of less than 6% at the highest incident energies, and less than 1% at the lowest energies. The $L_2(2P_{1/2})$ level gives up, at most, 13% of its initial vacancies, and this is approximately independent of energy. Finally, vacancy production in the $L_1(2S_{1/2})$ level was so small that Coster-Kronig transitions from this level were negligible. To summarize, effects of Coster-Kronig transitions on final vacancy distributions were found to be small and were neglected.

To obtain correct L -shell fluorescence yields for the target atoms, the number of vacancies produced in the $n=3$ shells of these atoms must be known. Since we do not have information concerning the number of these $n=3$ shell vacancies, to obtain vacancy-production rates from x-ray yields we used single-vacancy values of ω_L tabulated in Ref. 12. Calculations (Ref. 1) indicate that if the target atoms have less than eight vacancies in the $n=3$ shell at the time the L x ray is emitted, use of the single-vacancy fluorescence yields will introduce errors of less than 30% in the vacancy-production rates. If more than eight $n=3$ vacancies existed at the time of emission, errors of as much as a factor of two could result.

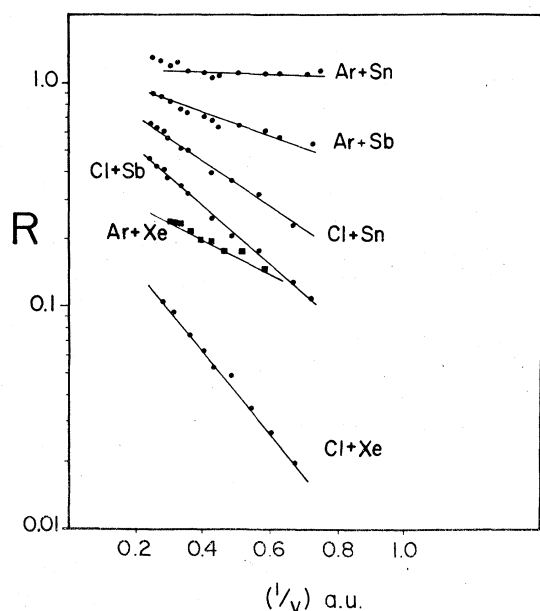


FIG. 3. Ratio R of the $2P_{3/2}$ vacancy-production cross section to the K -shell vacancy-production cross section for various collision systems, as a function of $1/v$, where v is the velocity, in atomic units, of the incident ion. The solid lines through the experimental points are estimated fits to the data. Statistical uncertainties in the data are 5% or less.

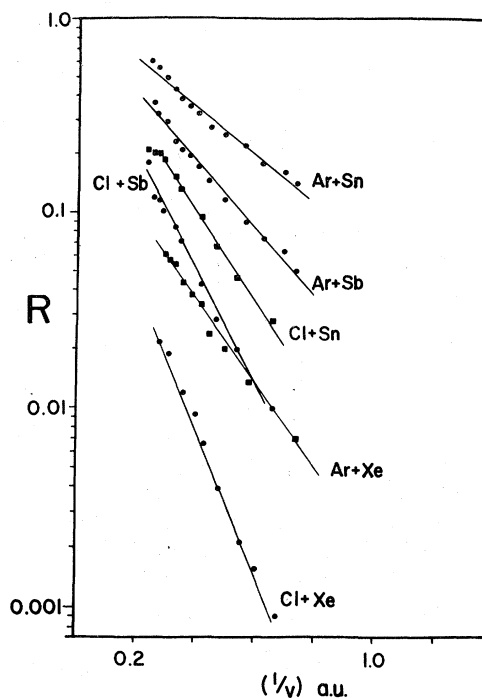


FIG. 4. Ratio R of the $2P_{1/2}$ vacancy-production cross section to the K -shell vacancy production cross section for various collision systems, as a function of $1/v$, where v is the velocity, in atomic units, of the incident ion. The solid lines through the experimental points are estimated fits to the data. Statistical uncertainties in the data are approximately 10%.

Experimental results are presented in Figs. 3 and 4. We plot, on a logarithmic scale, the ratio R , the cross section for production of vacancies in the L_2 or L_3 levels of target atoms divided by cross section for production of vacancies in the K shell in projectiles, as a function of the reciprocal of the velocity, in atomic units, of the projectile. Statistical uncertainties in the $L_3(P_{3/2})$ data are less than 5% and for the $L_2(P_{1/2})$ data are about 10%. As mentioned above, all of the $P_{1/2}$ points could be low by an amount equal to or less than 13%, because Coster-Kronig transitions out of the $P_{1/2}$ state were neglected. However, this error will not significantly affect the slopes of curves through the $P_{1/2}$ results. The solid curves are reasonable straight-line representations of the data.

III. DISCUSSION

As can be seen from Figs. 3 and 4, when the ratio of L to K vacancies is plotted on a logarithmic scale as a function of the reciprocal of the velocity of the incident ions, the data are reason-

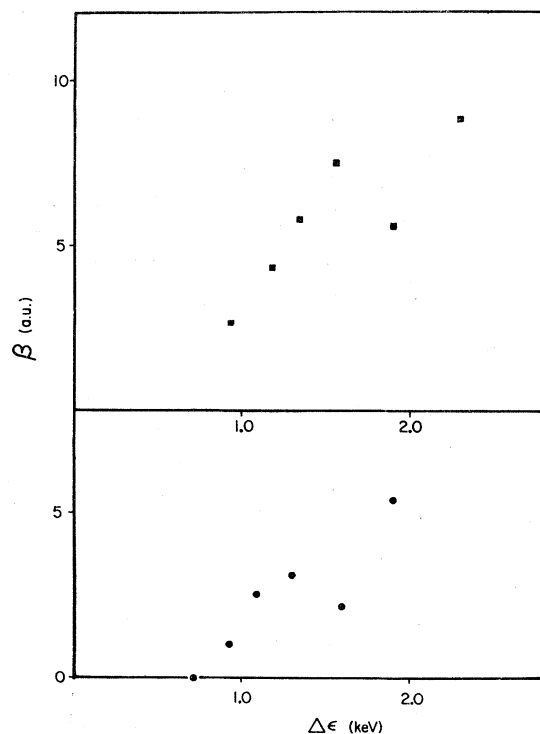


FIG. 5. Parameter β from the equation $R = Ae^{-\beta/v}$, in atomic units, as a function of $\Delta\epsilon$, the difference in binding energy of the two sharing levels in keV. The upper curve is the ratio for vacancies in the $2P_{1/2}$ levels of the heavy target atoms and the K shells of the projectiles, and the lower curve is for vacancies in the $2P_{3/2}$ levels and K shells.

ably well fit by straight lines. That is, the data can be fitted by the equation

$$R = Ae^{-\beta/v}, \quad (1)$$

and a different β results for each collision system. For all of the data which were obtained with solid targets, the most reasonable lines through the experimental points have intercepts at $1/v = 0$ of close to unity. It can also be seen from Figs. 3 and 4 that the straight lines through the gas-target data have intercepts between 0.25 and 0.4. It is possible that the gas-target curves have intercepts different from the solid-target curves because they have different L -shell fluorescence yields. Differences in fluorescence yields of excited atoms in solid and in gas targets have been observed previously.¹⁵

The values of β in Eq. (1) obtained from the curves in Figs. 3 and 4 are plotted in Fig. 5 as a function of $\Delta\epsilon$, the difference in the neutral-atom K - and L -binding energies of the partners in the

collision. As can be seen, there is some correlation between β and $\Delta\epsilon$.

Finally, we have attempted to interpret our data in terms of a two-state vacancy-sharing process. The united-atom separated-atom quasimolecular correlation rules of both Barat and Lichten⁵ and Eichler *et al.*⁹ indicate that the vacancies being shared between target L subshells and projectile K shells are initially produced in the rising $3d\sigma$ molecular orbital (see Fig. 2). As the collision partners separate, these vacancies can end up either in the projectile $1s$ state or they can be radially coupled to σ states that connect to the $2P_{3/2}$, $2P_{1/2}$, or $2S_{1/2}$ levels in the target atom. Nikitin⁷ has proposed a general two-state calculation based on a long-range exponential coupling model. His expression for the vacancy-sharing ratio R between any two radially coupled molecular orbitals can be written

$$R = \sigma_L/\sigma_K = [e^{2x(1+\cos\theta)} - 1]/[e^{4x} - e^{2x(1+\cos\theta)}]. \quad (2)$$

In this expression we have used the relation for x proposed by Meyerhof,³ namely

$$x = \pi(I_H^{1/2} - I_L^{1/2})/(2m)^{1/2}v,$$

where I_H and I_L are the ionization energies, respectively, of the L subshell of the heavy target and the K shell of the light projectile, m is the mass of the electron, and v is the velocity of the incident projectile. We then varied θ to obtain the most reasonable fits of our data to Eq. (2). Results of these comparisons are shown in Figs. 6(a) and 6(b). The solid curves are plots of Eq. (2) for the values of θ indicated.

As can be seen in Fig. 6(b), ratios of vacancies in $L_2(2P_{1/2})$ levels of the target atoms to those in the K shells of the projectiles are reasonably well described by Eq. (2), with values of $\theta = 60^\circ$ and 70° . Meyerhof *et al.*⁶ fit their $L_2(2P_{1/2})$ data with values of $\theta = 72^\circ$ and 85° . The $L_3(2P_{3/2})$ to K -vacancy ratios illustrated in Fig. 6(a) are only poorly described. Data for argon on xenon, and chlorine on xenon, antimony and tin are mainly between the curves for $\theta = 50^\circ$ and 60° . However, no value of θ fits the curves for argon on tin and antimony. In fact, no reasonable values of x and θ could be found which would fit the argon on tin and antimony $L_3(2P_{3/2})$ data. Qualitatively, it appears that our data are progressively less well fit as $\Delta\epsilon$, the separated-atom energy difference between the sharing levels, becomes smaller. Meyerhof *et al.*⁶ obtain results of $\theta = 54^\circ$ and 76° from their $L_3(2P_{3/2})$ data.

This lack of agreement for small $\Delta\epsilon$ may indicate a weakness in the theory, or perhaps more likely, may show that a two-level theory such as that of Nikitin, cannot be expected accurately to

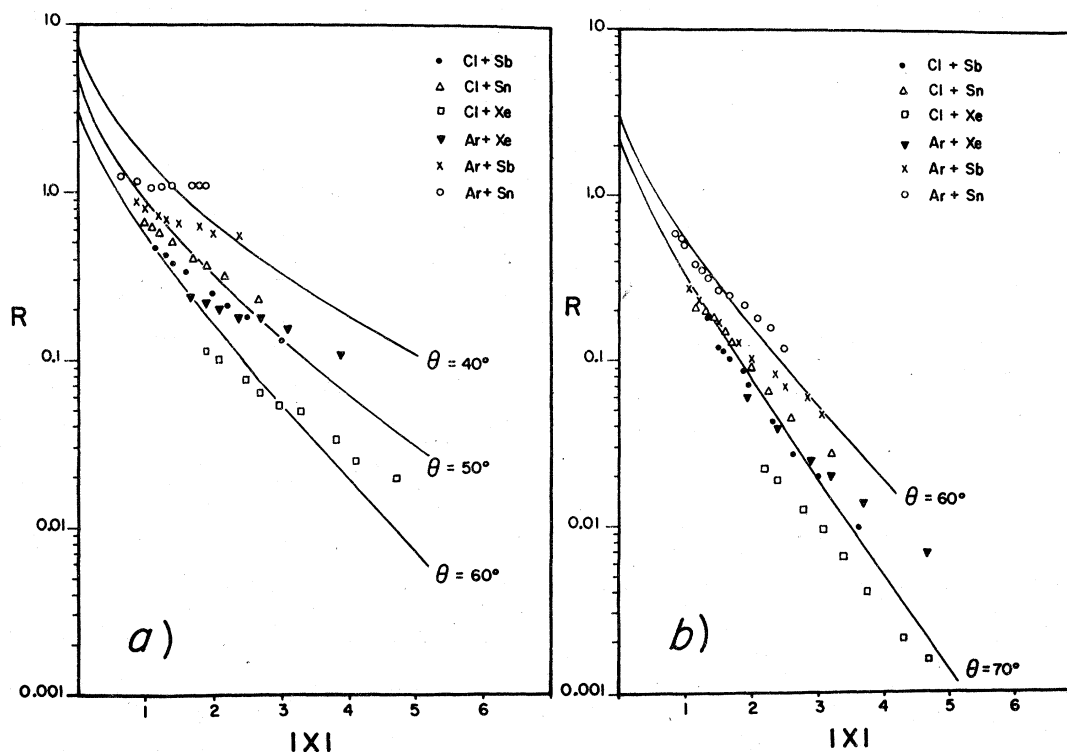


FIG. 6. Measured vacancy-sharing ratios R versus the parameter $|x|$ discussed in the text. The solid curves are plots of the ratios calculated from the two-state theory of Nikitin. Curve (a) gives the $2P_{3/2}$ data, and curve (b), the $2P_{1/2}$ data.

describe results obtained with a system, such as those used in this experiment, where at least three states can be participating in the physical processes.

ACKNOWLEDGMENTS

The authors thank Professor W. E. Meyerhof for several very helpful comments concerning this

work. We also acknowledge many conversations with Professor J. D. Garcia concerning all phases of this work. Finally, we would like to thank Peter Stoss for his many years of service in maintaining and operating the University of Arizona Van de Graaff Accelerator. This work was supported in part by grants from NSF and ONR.

*Present address: Bell Laboratories, Holmdel, N. J. 07733.

[†]On leave from Western Michigan University, Kalamazoo, Mich. 49008.

¹J. D. Garcia, R. J. Fortner, and T. M. Kavanagh, *Rev. Mod. Phys.* **45**, 111 (1973).

²H. Kubo, F. C. Jundt, and K. H. Purser, *Phys. Rev. Lett.* **31**, 674 (1973).

³W. E. Meyerhof, *Phys. Rev. Lett.* **31**, 1341 (1973).

⁴Yu. N. Demkov, *Sov. Phys.-JETP* **18**, 138 (1964).

⁵M. Barat and W. Lichten, *Phys. Rev. A* **6**, 211 (1972).

⁶W. E. Meyerhof, R. Anholt, J. Eichler, and A. Salop, *Phys. Rev. A* **17**, 108 (1978).

⁷E. E. Nikitin, in *Advances in Quantum Chemistry*, edited by P. O. Löwdin (Academic, New York, 1970),

Vol. 5, p. 135.

⁸E. M. Middlesworth, Jr., D. J. Donahue, L. C. McIntyre, Jr., and E. M. Bernstein, *Phys. Rev. A* **17**, 141 (1978).

⁹J. Eichler, U. Willie, B. Fastrup, and K. Taulbjerg, *Phys. Rev. A* **14**, 707 (1976).

¹⁰James H. Scofield, *Phys. Rev.* **179**, 9 (1969).

¹¹W. J. Veigele, *At. Data Tables* **5**, 51 (1973).

¹²W. Bambynek, B. Crasemann, R. W. Fink, H. V. Freund, R. E. Price, and P. V. Rao, *Rev. Mod. Phys.* **44**, 716 (1972).

¹³E. J. McGuire, *Phys. Rev.* **185**, 1 (1969).

¹⁴F. P. Larkins, *J. Phys. B* **4**, 129 (1971).

¹⁵R. C. Der, R. J. Fortner, T. M. Kavanagh, and J. M. Khan, *Phys. Rev. A* **4**, 556 (1971).